A harmonic model for the temporal variation of lightning activity over Africa

A. B. Collier[1,2] and A. R. W. Hughes[2]

Received 29 June 2010; revised 16 November 2010; accepted 7 December 2010; published 4 March 2011.

[1] Concise rainfall, temperature, and humidity climatologies are available for most countries, reflecting the regular annual variation of these quantities, usually with monthly resolution. Although numerous surveys of global and regional lightning activity exist, no comparable national climatologies of lightning activity are available. Annual lightning flash rate patterns for most African countries are derived here using 10 years of data from two satellite lightning detectors. These patterns can be represented accurately by annual and semiannual sinusoidal components superimposed on a mean level. The highest-average lightning activity (47.8 km^{-2} yr^{-1}) occurs in the Democratic Republic of the Congo, while the lowest (0.2 km^{-2} yr^{-1}) is found in Egypt. Very little lightning is observed in the Sahara, while a consistently high intensity is found throughout the tropics. There is a clear reversal in the phase of the annual component across the equator. Within the tropics the amplitude of the semiannual variation is a significant fraction of that of the annual variation but becomes less important in the subtropics.

Citation: Collier, A. B., and A. R. W. Hughes (2011), A harmonic model for the temporal variation of lightning activity over Africa, *J. Geophys. Res.*, *116*, D05105, doi:10.1029/2010JD014455.

1. Introduction

[2] The distribution of terrestrial lightning varies with both location and time. The mean global flash rate of 44 s^{-1} [*Christian et al.*, 2003] is not uniformly distributed across the globe. Lightning activity over land outweighs that over the ocean by a factor of roughly 8 [*Christian et al.*, 2003], with the majority occurring in the tropics [*Orville and Henderson*, 1986]. Peak flash rates in the Northern Hemisphere exceed those in the Southern Hemisphere, so that maximum global lightning activity is achieved during the Boreal summer [*Christian et al.*, 2003].

[3] Lightning activity exhibits temporal variations over diurnal, intraseasonal, semiannual, annual and interannual time scales [*Williams*, 1992; *Sátori and Zieger*, 1996; *Füllekrug and Fraser-Smith*, 1997; *Nickolaenko et al.*, 1999]. The amplitudes of the semiannual and annual variations may be as large as 50% and 50–100%, respectively, of the mean [*Williams*, 2005, Table 1]. In both hemispheres the annual variation is driven principally by the seasons: in general it is highest during the summer, lowest during the winter and transitions around the equinoxes. Tropical lightning activity is focused over three chimney regions [*Williams and Sátori*, 2004] and has a distinct semiannual variation. The semiannual signal from tropical Africa is roughly symmetric around the solstices, while the signals from South America and the Maritime Continent are biased toward the autumnal and vernal equinoxes, respectively [*Christian et al.*, 2003]. The diurnal pattern in lightning activity is most apparent over land, where there is generally a peak in the late afternoon [e.g., *Collier et al.*, 2006]. Oceanic lightning does not exhibit an obvious diurnal variation.

1.1. Association With Other Phenomena

[4] There is a strong association between lightning and precipitation [e.g., *Carte and Kidder*, 1977; *Soula and Chauzy*, 2001]. The seasonal variation in lightning is of interest due to the intense rainfall associated with thunderstorms, which is important for agriculture but may also be destructive, resulting in flash floods.

[5] Lightning can also be potentially harmful for technology, industry and life. An appreciable portion of the associated damage is due to fires initiated by lightning [*Krider et al.*, 1980; *Rorig and Ferguson*, 2002]. Lightning accounts for a number of injuries and fatalities [*Coates et al.*, 1993; *Curran et al.*, 2000; *Elsom*, 2001], and is responsible for more loss of life than other natural hazards. It is, however, underrated due to the isolated nature of the incidents. The global annual fatality rate due to lightning is between 0.2 and 1.7 per million people [*Wetli*, 1996], the frequency generally being larger in regions of greater lightning activity. The majority of recorded fatalities occurred in open spaces during summer afternoons. There has been a systematic decrease in the fatality rate due to lightning, which was attributed to the general migration of the population from rural to urban areas, more substantial buildings and greater awareness through education and forecasting [*López and Holle*, 1998; *Holle*, 2008]. It is probable that the reported number of injuries and fatalities due to lightning fall short of the true statistics [*López et al.*, 1993]. Within

[1]Hermanus Magnetic Observatory, Hermanus, South Africa.
[2]School of Physics, University of KwaZulu-Natal, Durban, South Africa.

0148-0227/11/2010JD014455

Africa there is a paucity of published data regarding lightning fatalities. The average annual death rates during the latter half of the twentieth century for South Africa and Zimbabwe are 1.5 and 13.4 per million people, respectively [*Coates et al.*, 1993, Table 2]. On the South African Highveld, a region of profuse lightning activity, 6.3 lightning related deaths were recorded per million people [*Blumenthal*, 2005]. *Dlamini* [2009] reported a fatality rate of 15.5 per million people in Swaziland, which is the highest rate in the world. The relatively high incidence of injury and fatality due to lightning in Africa suggests that a better understanding of the spatial and temporal variability of lightning incidence would be beneficial.

1.2. Relation to Atmospheric Conditions

[6] Temperature and water vapor are the dominant factors influencing the spatial and temporal distribution of thunderstorms. Warm, moist air provides the most conducive thermodynamic environment for convection and thundercloud formation. Warm air not only drives convection, but has a greater capacity for moisture than cooler air.

[7] The relationship between temperature and lightning is mediated by atmospheric buoyancy. The surface wet-bulb temperature, which embodies the effects of both temperature and moisture, appears to control the level of atmospheric instability [*Williams*, 1992; *Williams and Renno*, 1993]. Modest deviations from the ambient temperature violate hydrostatic equilibrium, causing convection. The intensity of the convection influences cloud electrification by regulating the collision frequency between graupel and ice [*Takahashi*, 1978; *Williams*, 1985]. The dependence of the electrification process on surface air temperature, updraft speed, liquid water content and cloud temperature is inherently nonlinear [*Saunders et al.*, 1991; *Williams*, 1992; *Baker et al.*, 1999]. This suggests that variations in global lightning activity may be a sensitive proxy for global tropospheric change [*Williams*, 1992; *Price and Rind*, 1994; *Bering*, 1995], although this relationship is not always readily observed [*Watkins et al.*, 2001].

[8] Changes in surface air temperature are regulated by the intensity of incident radiation from the Sun, and depend on the balance between incoming shortwave radiation and outgoing longwave radiation, both of which exhibit a 24 h periodicity. Diurnal heating is also controlled by the duration of solar illumination, which varies with season and latitude.

[9] The magnitude of the insolation cycle is determined by the Earth's orbital eccentricity and the obliquity of its rotation axis with respect to the ecliptic. During the course of the year the intensity of the solar radiation at 1 AU varies by 6.7%, with a maximum in January, due to a 3.4% change in the Earth-Sun distance. The obliquity of the Earth's axis results in seasonal modulation of insolation, which in turn modifies the surface temperature. The amplitude of the modulation increases with latitude, causing a semiannual variation in the tropics, with maxima near the equinoxes [*Williams*, 1994, Figure 3], and an annual variation at higher latitudes, with a maximum around the summer solstice. The semiannual pattern in the tropics is also reflected in the occurrence of thunderstorms [*Williams*, 1994, Figure 7].

[10] Solar insolation is not the only factor determining the occurrence of lightning. The presence of cloud condensation nuclei plays a role in initiating cloud formation. In order for clouds to accrete there must also be sufficient moisture. Relative humidity is thus a critical factor in thunderstorm formation. A lack of moisture implies no clouds, while a surfeit is more conducive to precipitation than lightning. An intermediate level of atmospheric moisture is thus preferable.

1.3. Rationale and Importance

[11] Changes in the distribution and intensity of lightning activity are likely to arise due to modifications in global temperature [*Dinnes*, 1999; *Williams*, 1992], but other factors, such as solar activity and cosmic ray flux, may also be influential. There have been reports of the influence of the solar cycle on lightning activity dating back to the work of *Brooks* [1934]. Although there is some skepticism regarding a plausible link between solar activity and weather [*Pittock*, 1978], there is evidence to suggest that both solar radiative forcing [*Bengtsson*, 2006] and the modulation of cosmic rays [*Marsh and Svensmark*, 2000; *Carslaw et al.*, 2002] exert an influence on climate. The latter effect remains a contentious issue since *Calogovic et al.* [2010] found that no change in global cloud cover was associated with Forbush decreases in cosmic ray flux. The El Niño-Southern Oscillation (ENSO) has an influence on precipitation anomalies over Equatorial [*Misra*, 2010] and Southern [*Reason and Rouault*, 2002] Africa, and is also likely to affect the incidence of lightning in this region. Recently it has been suggested that lightning over Africa may provide the seed for hurricanes and tropical storms on the east coast of the United States [*Price et al.*, 2007]. A tantalizing link appears to exist between all of these phenomena [*Goldenberg and Shapiro*, 1996]. However, in order to study these connections, a detailed knowledge of the normal or average variation in lightning occurrence must be established against which deviations can be measured. *Christian et al.* [2003, Figures 7–9] presented reference curves for broad zonal and meridional bands, but such statistics are required over regional scales.

2. Data and Analysis

[12] The lightning data presented here represent statistics pertaining to countries in Africa. Only countries with areas greater than 0.01 Mm^2 are considered in this analysis since the sampling statistics for smaller countries are too poor. This leaves 48 countries with areas from 0.011 Mm^2 (Gambia) to 2.511 Mm^2 (Sudan).

2.1. Lightning Data

[13] The Optical Transient Detector (OTD) and Lightning Imaging Sensor (LIS) are two satellite borne lightning detectors which use narrow band infrared filters and sophisticated image processing techniques to identify the time and location of lightning discharges. As opposed to some terrestrial lightning detection systems, the optical lightning location technique employed by LIS/OTD identifies discharges of all orientations, and thus includes cloud-to-ground (CG), intracloud (IC) and cloud-to-cloud (CC) flashes.

[14] Data from both OTD and LIS are available in a variety of formats. The 0.5° High Resolution Annual Climatology (HRAC) version 2.2 gridded LIS/OTD data were used in this analysis. The data represent a synthesis of the 5 year OTD

(May 1995 to April 2000) and 8 year LIS (January 1998 to December 2005) sets [*Boccippio et al.*, 2002; *Christian et al.*, 2003]. The data from the two instruments have been intercalibrated to obtain consistency. The gridded data products are generally preferable for a time series analysis since they incorporate the appropriate spatial and temporal variations in detection efficiency. The HRAC data have daily temporal resolution but each measurement represents a ~110 day centered moving average, reducing the effect of diurnal aliasing. The smoothed rates are formed by independently averaging the aggregated flash counts and view times over the ~110 day period and then dividing to obtain the rate. The variance of the data is further improved by averaging over a number of years to form an annualized climatology. The data are also spatially smoothed with a 2.5° moving average.

[15] The HRAC data were spatially partitioned to form an annualized time series at daily resolution for each country under consideration. A 0.5° × 0.5° cell in the HRAC data was allocated to a particular country if the centroid of the cell fell within the borders of that country. Therefore, along the borders of neighboring countries, grid cells may effectively cover regions from both countries but the corresponding data is only assigned to the country incorporating the centroid. Similarly, along coastlines the discrete nature of the grid can result in some coastal lightning being assigned to a country or, conversely, some continental lightning being neglected depending on the location of the cell centroid with respect to the coastline. The effects of the former are not particularly important for this analysis because, although intense lightning may occur over the oceans [*Füllekrug et al.*, 2002; *Price et al.*, 2007], continental lightning discharges outnumber those over the oceans by a factor of around 10:1 [*Christian et al.*, 2003]. Due to the nature of the gridded data, it was not possible to assess the lacunarity and the fraction of each country's area which was affected by thunderstorm activity was thus not determined.

[16] Examples of the resulting data for a selection of countries are presented in Figure 1. In the upper panel of each plot the solar declination, δ, is compared to the respective country's centroid latitude. Maximum solar heating is expected when the solar declination corresponds to the latitude of a location on the surface of the Earth.

[17] The data in Figure 1 indicate that there is an appreciable diversity in the annualized pattern of lightning activity. Some countries, like South Africa and Sudan, have a simple pattern, while others, like Sierra Leone and Liberia, are somewhat more elaborate. The patterns are consistent with the seasons in the two hemispheres. Whereas a country well south of the equator, such as South Africa, exhibits a peak at the beginning of the year, a country well north of the equator, such as Mali, has a midyear peak. Countries close to the equator, for example Liberia and Sierra Leone, have two maxima during the year. This might immediately be attributed to the fact that the Sun approaches the zenith twice during the year at low latitudes.

[18] Although the annualized national patterns in Africa broadly conform to the classes mentioned above, which class applies to a given country is not always obvious. The unimodal curve for South Africa is typical of other countries similarly located, and persists farther north, as far as Zambia and Malawi, both of which are well within the tropics. Close to the equator, however, the pattern departs from a strictly annual variation, becoming distinctly bimodal. Progressing farther into the Northern Hemisphere the two peaks come closer together until they coalesce into a single peak once more. Some countries which have a large latitudinal extent exhibit a composite of both behaviors. The Democratic Republic of the Congo, for example, experiences intense lightning from November until March, which is the superposition of two peaks originating close to the equator and a single peak from farther south.

2.2. Sinusoidal Fit

[19] Most geophysical data embody some degree of persistence [*Dmowska and Saltzman*, 1999]. Certainly this is apparent in precipitation over central Africa, where the average decorrelation time generally exceeds 4 days [*Misra*, 2010]. Persistence of precipitation is sustained by local surface evaporation. In the tropics a similar mechanism applies to lightning: if there is a thunderstorm on a given day then the resulting precipitation leads to humid conditions the following day, which are conducive to the production of another thunderstorm. This does not apply in the subtropics where large-scale atmospheric systems, like the African Easterly Wave (AEW), are dominant [*Chronis et al.*, 2006]. Numerous approaches exist for evaluating the level of persistence [e.g., *Mudelsee*, 2002]. The duration of persistence is not indefinite and it is apparent from lightning data that active periods are interspersed with inactive intervals, yielding a somewhat irregular variation in lightning activity. However, averaging the variations for a number of years produces smooth patterns like those presented in Figure 1.

[20] *Collier et al.* [2006] observed that the variation of the flash rate within a region off the east coast of South Africa was well described by a sinusoid with a period of 1 year. The data in Figure 1i indicate that this applies to South Africa as a whole. It is, however, also apparent from the remaining plots in Figure 1 that the simple monochromatic sinusoidal variation does not extend well to all other countries, especially those at low latitudes. In order to achieve a reasonable fit to these data it is necessary to include a semiannual variation as well. The semiannual component was previously identified in data reflecting thunderstorm days at tropical stations and was found to be in phase with the temperature maxima [*Williams*, 1994].

[21] A harmonic model was applied to the annualized data for the countries under consideration. The model was of the form

$$S = \alpha + \gamma_1 \cos 2\pi(t - \phi_1) + \gamma_2 \cos 4\pi(t - \phi_2), \qquad (1)$$

where the parameters α and γ have units of flashes km^{-2} yr^{-1}, while the phase shift, ϕ, and time, t, are dimensionless and represent fractions of a year. The constant term, α, reflects the average level of activity throughout the year, while the remaining terms constitute the annual and semiannual variations. There is no danger of over fitting in such a simplistic model: there are sufficient parameters to capture the important features, yet not enough to produce artificially small residuals (specific random features in the data are not reflected in the model). A nonlinear least squares fitting routine was employed to estimate appropriate values for the parameters. The derived parameters are presented in

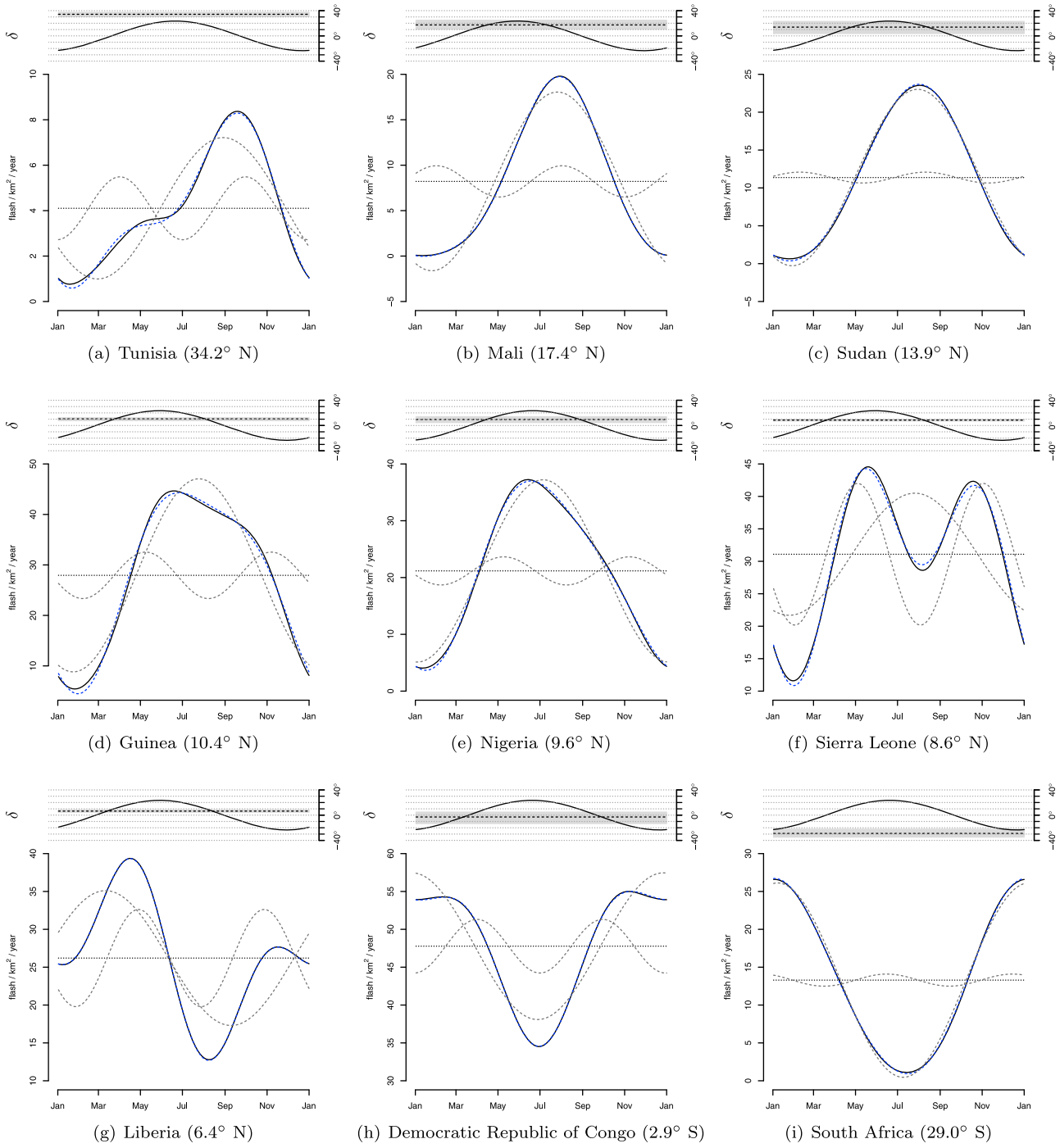

(a) Tunisia (34.2° N) (b) Mali (17.4° N) (c) Sudan (13.9° N)

(d) Guinea (10.4° N) (e) Nigeria (9.6° N) (f) Sierra Leone (8.6° N)

(g) Liberia (6.4° N) (h) Democratic Republic of Congo (2.9° S) (i) South Africa (29.0° S)

Figure 1. Annualized total flash rate density for a selection of countries constructed from 10 years of LIS/OTD data. The mean latitude, $\overline{\lambda}$, is specified in parentheses in each plot label. The data are plotted as a solid black curve; the annual and semiannual components of a sinusoidal fit are dashed in grey, while their sum is dashed in blue. The top panel in each plot reflects the solar declination, δ, determined at midday, with a horizontal dashed line at the respective country's centroid latitude and a shaded region indicating the latitudinal extent of the country.

Table 1. Although it is possible to decompose an arbitrary signal into the sum of a sufficient number of sinusoidal components, it is apparent from the small residual standard errors, σ, that only the first two harmonics included in equation (1) are required to produce an excellent representation of the data. It is important to note that a small σ indicates that the model is a good fit to the data but does not reflect the quality of the underlying data. This is really only a concern in the case of Egypt where lightning is so rare that the pattern derived from the data is spurious.

Table 1. Parameters Describing the Variation of Total Lightning Flash Rate[a]

	Country	Area (Mm^2)	α	γ_1	ϕ_1	γ_2	ϕ_2	γ_2/γ_1	$\Delta\phi$	σ
AGO	Angola	1.24	19.5	15.2	30/12 [364]	3.4	12/10 [285]	0.23	−0.22	0.283
BDI	Burundi	0.03	23.9	13.5	09/01 [009]	3.0	09/03 [068]	0.22	0.16	0.229
BEN	Benin	0.12	19.0	14.3	28/06 [179]	2.3	06/05 [126]	0.16	−0.14	0.204
BFA	Burkina Faso	0.28	16.1	17.6	11/07 [192]	1.3	04/07 [185]	0.07	−0.02	0.177
BWA	Botswana	0.58	11.6	12.1	03/01 [003]	1.4	13/12 [347]	0.12	−0.06	0.102
CAF	Central African Republic	0.62	32.0	21.1	14/07 [195]	4.4	24/04 [114]	0.21	−0.22	0.413
CIV	Côte d'Ivoire	0.32	20.0	7.9	13/05 [133]	4.0	29/04 [119]	0.51	−0.04	0.098
CMR	Cameroon	0.47	30.6	12.2	24/06 [175]	6.7	23/04 [113]	0.55	−0.17	0.143
COD	Democratic Republic of the Congo	2.34	47.8	9.7	26/12 [360]	3.5	29/09 [272]	0.37	−0.24	0.064
COG	Republic of the Congo	0.34	40.6	17.9	01/02 [032]	3.8	08/04 [098]	0.21	0.18	0.259
DJI	Djibouti	0.02	7.9	7.6	08/08 [220]	2.2	13/09 [256]	0.29	0.10	0.181
DZA	Algeria	2.32	2.0	2.1	03/08 [215]	0.4	01/09 [244]	0.17	0.08	0.045
EGY	Egypt	0.98	0.2	0.0	23/11 [327]	0.1	21/10 [294]	6.81	−0.09	0.006
ESH	Western Sahara	0.27	1.0	1.1	26/08 [238]	0.4	31/08 [243]	0.34	0.02	0.026
ETH	Ethiopia	1.26	12.4	10.4	14/07 [195]	1.2	25/08 [237]	0.11	0.11	0.106
GAB	Gabon	0.27	32.8	22.2	08/02 [039]	5.1	18/04 [108]	0.23	0.19	0.425
GHA	Ghana	0.24	21.2	8.5	24/05 [144]	4.3	27/04 [117]	0.51	−0.07	0.178
GIN	Guinea	0.25	27.9	19.1	24/07 [205]	4.6	07/05 [127]	0.24	−0.21	0.684
GMB	Gambia	0.01	8.1	10.2	12/08 [224]	1.8	15/08 [227]	0.18	0.01	0.216
GNB	Guinea-Bissau	0.03	18.2	19.2	21/08 [233]	2.1	05/10 [278]	0.11	0.12	0.746
GNQ	Equatorial Guinea	0.02	31.0	19.5	14/02 [045]	5.5	20/04 [110]	0.28	0.18	0.549
KEN	Kenya	0.58	3.8	1.4	18/03 [077]	0.7	02/04 [092]	0.52	0.04	0.050
LBR	Liberia	0.10	26.2	8.9	10/03 [069]	6.4	27/04 [117]	0.72	0.13	0.039
LBY	Libya	1.62	0.4	0.3	10/08 [222]	0.1	07/10 [280]	0.29	0.16	0.010
LSO	Lesotho	0.03	23.8	24.5	13/01 [013]	2.1	17/01 [017]	0.08	0.01	0.134
MAR	Morocco	0.40	3.2	2.7	24/07 [205]	0.4	17/09 [260]	0.16	0.15	0.067
MDG	Madagascar	0.59	16.9	18.6	04/01 [004]	2.7	14/12 [348]	0.14	−0.06	0.282
MLI	Mali	1.25	8.2	9.8	25/07 [206]	1.7	01/08 [213]	0.17	0.02	0.055
MOZ	Mozambique	0.79	9.6	11.5	10/01 [010]	2.4	05/01 [005]	0.21	−0.01	0.066
MRT	Mauritania	1.04	2.7	3.3	10/08 [222]	0.9	19/08 [231]	0.29	0.03	0.050
MWI	Malawi	0.12	11.7	14.9	16/01 [016]	3.0	16/01 [016]	0.20	0.00	0.069
NAM	Namibia	0.83	7.9	7.9	17/01 [017]	0.3	12/02 [043]	0.03	0.07	0.086
NER	Niger	1.19	4.7	6.4	26/07 [207]	1.7	29/07 [210]	0.27	0.01	0.068
NGA	Nigeria	0.91	21.2	16.0	05/07 [186]	2.5	08/05 [128]	0.15	−0.16	0.333
RWA	Rwanda	0.03	20.9	6.9	06/12 [340]	2.1	11/09 [254]	0.31	−0.24	0.207
SDN	Sudan	2.51	11.4	11.6	29/07 [210]	0.7	09/08 [221]	0.06	0.03	0.142
SEN	Senegal	0.20	8.0	9.7	10/08 [222]	1.5	13/08 [225]	0.16	0.01	0.179
SLE	Sierra Leone	0.07	31.1	9.4	25/07 [206]	10.9	03/05 [123]	1.16	−0.23	0.571
SOM	Somalia	0.63	1.7	1.3	07/05 [127]	0.9	23/04 [113]	0.65	−0.04	0.063
SWZ	Swaziland	0.02	16.6	16.4	25/12 [359]	2.7	12/12 [346]	0.16	−0.04	0.234
TCD	Chad	1.27	9.4	11.3	28/07 [209]	1.8	30/07 [211]	0.16	0.01	0.058
TGO	Togo	0.06	21.3	10.0	03/07 [184]	3.8	15/04 [105]	0.38	−0.21	0.242
TUN	Tunisia	0.15	4.1	3.1	28/08 [240]	1.4	29/09 [272]	0.44	0.09	0.118
TZA	United Republic of Tanzania	0.94	10.6	11.4	27/01 [027]	2.3	06/02 [037]	0.20	0.03	0.070
UGA	Uganda	0.24	22.1	5.7	27/08 [239]	2.1	25/09 [268]	0.36	0.08	0.118
ZAF	South Africa	1.22	13.3	12.8	07/01 [007]	0.8	14/12 [348]	0.06	−0.07	0.108
ZMB	Zambia	0.75	14.8	17.0	07/01 [007]	1.8	30/12 [364]	0.10	−0.02	0.254
ZWE	Zimbabwe	0.39	9.6	11.4	30/12 [364]	2.0	19/12 [353]	0.18	−0.03	0.145

[a]The parameters α and γ have units of flashes km^{-2} yr^{-1}. For ease of interpretation the phase, ϕ, has been expressed in a form which reflects the location of the peak of the respective waveform (format: dd/mm [jjj], where dd is day in month, mm is month and jjj is day in year). The relative phase, $\Delta\phi$, indicates the fraction of a year by which the peak in the annual curve precedes ($\Delta\phi > 0$) or follows ($\Delta\phi < 0$) the nearest peak in the semiannual curve. The quality of the fit is indicated by σ, the residual standard error based on 360 degrees of freedom. The quoted areas are the effective values used to calculate the flash rate densities.

2.3. Annual Mean

[22] Figure 2 displays the geographical distribution of the average annual flash rate, α. These rates compare favorably with the results of *Christian et al.* [2003, Figure 4]. The countries with the highest and lowest mean annual flash rates are the Democratic Republic of the Congo (47.8 km^{-2} yr^{-1}) and Egypt (0.2 km^{-2} yr^{-1}), respectively.

[23] *Kuleshov et al.* [2006] compared ground-based lightning flash measurements at 39 sites in Australia to the corresponding flash rate densities derived from LIS/OTD data, finding that the two data sets agreed to within ±12%, with the satellite measurements generally exceeding those made on the ground. The values of α from Table 1 were compared to those calculated by *Christian et al.* [2003] for various locations in Africa. The disparity is at most −74.7% and, with the exception of one marginal location, *Christian et al.*'s [2003] values always exceed α. However, the values of α represent averages over entire countries, while the *Christian et al.* [2003] data were essentially point measurements at locations which had intense lightning activity, so that this bias was to be anticipated. The trend of diminishing α toward higher latitudes agrees with *Mackerras and Darveniza* [1994, Figure 2], although their results also reflect local lightning activity within only 12–16 km of the detectors. Values of α might be assumed to underestimate the actual flash rate density quite significantly at particular locations where lightning is profuse, in which case error

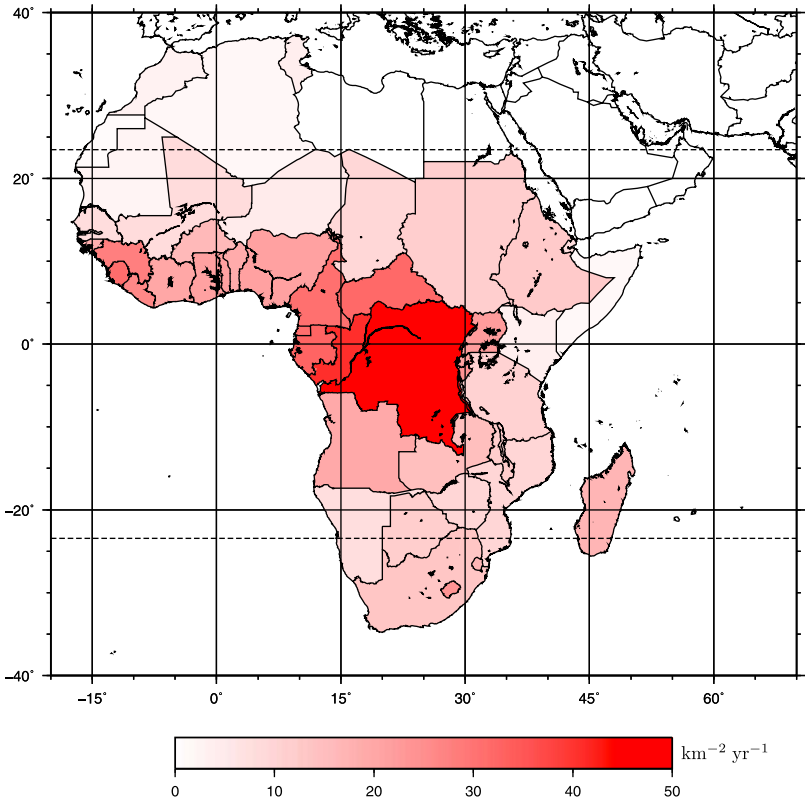

Figure 2. Values of the mean annual total flash rate, α.

estimates of around 50% might be appropriate. In contrast, *Jayaratne and Ramachandran* [1998], using ground-based lightning observations, found that the annual mean flash rate density in the vicinity of Gaborone, Botswana was 13.3 km^{-2} yr^{-1}, which compares favorably with the average for Botswana of α = 11.6 km^{-2} yr^{-1}.

2.4. Amplitude

[24] It is apparent from Table 1 that, with a few notable exceptions like Egypt and Sierra Leone, the model is dominated by the annual cycle. The mean amplitudes of the annual and semiannual components are 11.0 and 2.5 km^{-2} yr^{-1}, respectively. Figures 3 and 4 reflect the amplitude and phase of the annual and semiannual components.

[25] The presence of a semiannual cycle only induces two distinct maxima in lightning activity when the amplitude of this cycle is appreciable with respect to that of the annual cycle. *Williams* [2009] noted that the presence of a semiannual signal only becomes apparent once its amplitude exceeds one quarter of the amplitude of the annual signal, which corresponds to $\gamma_2/\gamma_1 > 0.25$. The ratio γ_2/γ_1 is tabulated in Table 1. In general γ_2 is significantly smaller than γ_1, although there are exceptions: Liberia and Somalia, which have $\gamma_2/\gamma_1 \approx 1$, exhibit a well defined bimodal pattern, while Sierra Leone has $\gamma_2/\gamma_1 > 1$ and is dominated by the semiannual component. Although Egypt also has $\gamma_2/\gamma_1 \gg 1$, this is not significant since in this case the amplitudes of both components are too small to be meaningful. The largest values of γ_2 are found in West Africa, in a region in which the annual weather pattern is modulated by the motion of the Intertropical Convergence Zone (ITCZ), which forms part of the large-scale tropical circulation. Outside the tropics the values of γ_2 are negligible.

[26] Considering the annual variation, it is evident from Figure 3a that the largest variations occur close to the equator and in small countries like Lesotho and Swaziland. The Democratic Republic of the Congo has an annual variation with an amplitude significantly smaller than the annual mean so that there is an appreciable level of lightning activity throughout the year. The median of the ratio γ_1/α is 0.93, indicating that for most countries the annual variation is such that lightning activity virtually disappears at some stage during the year.

2.5. Phase

[27] The relative phase, $\Delta\phi$, listed in Table 1 indicates the phase of the semiannual component relative to the peak in the annual curve. When $\Delta\phi \sim 0$, the annual peak is sharpened by the semiannual curve. Furthermore, in this case, although the positive peaks of the annual and semiannual variation are in phase, the negative peak of the annual component occurs at the same time as a positive peak in the semiannual component, which serves to flatten the annual trough, satisfying the constraint that the flash rate cannot be negative during the winter months [*Hsu and Wallace*, 1976]. This effect is apparent in Figure 1b. When $\Delta\phi \sim \pm 0.25$, the peak in the annual variation is accompanied by a trough in the semiannual signal, which serves to depress the main peak. This effect is illustrated in Figures 1d and 1h.

[28] The spatial distributions of ϕ_1 and ϕ_2 are also presented in Figures 3 and 4. In Figure 3b, there is a dramatic reversal in the phase of the annual variation across the

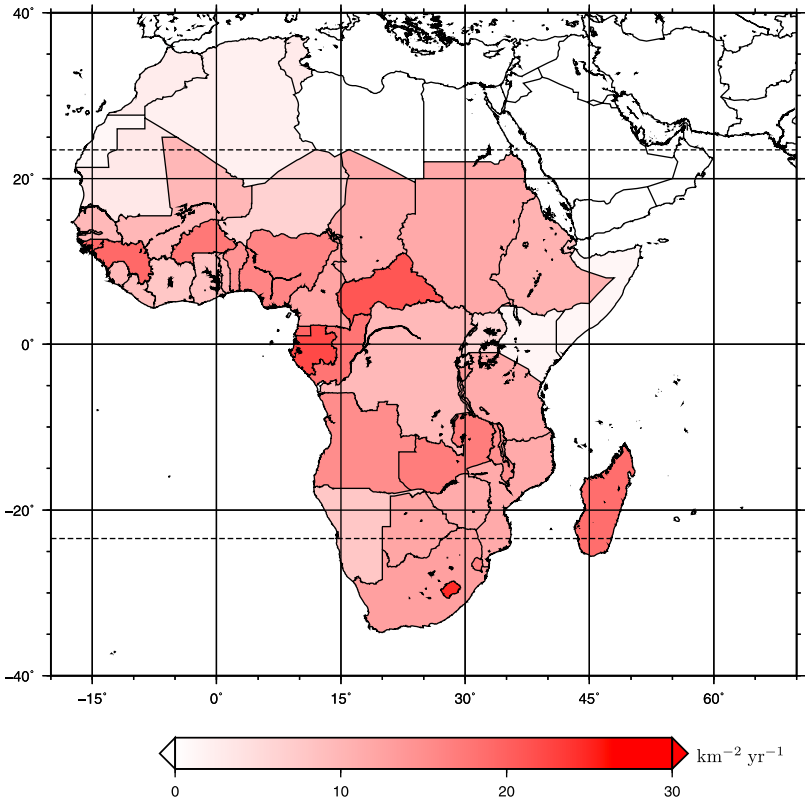

(a) amplitude, γ_1

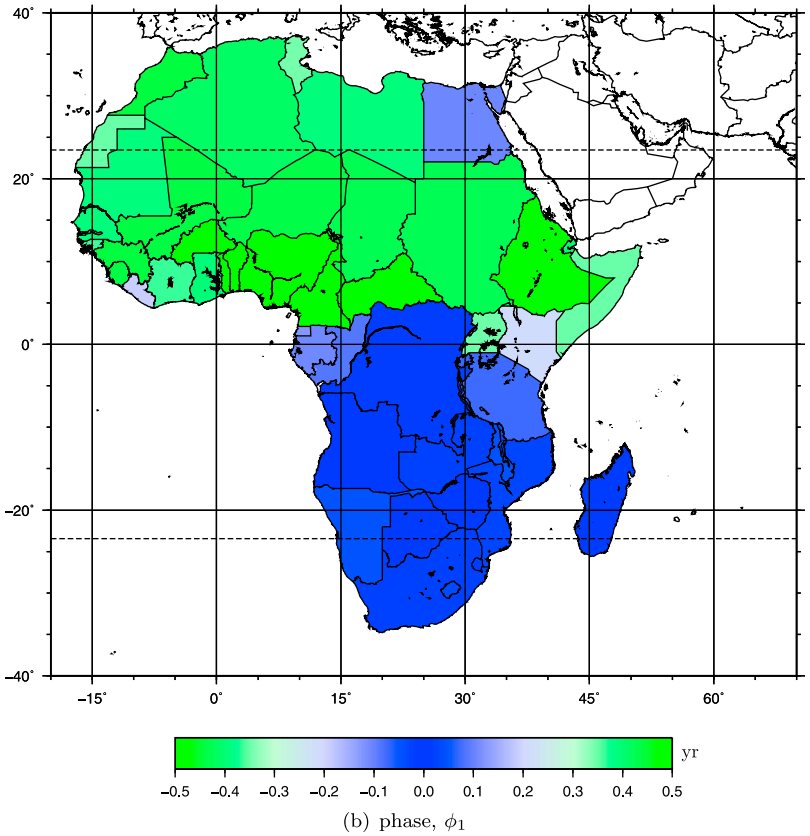

(b) phase, ϕ_1

Figure 3. Parameters for the annual component of total flash rate. The phase is in units of 1 year centered on 1 January.

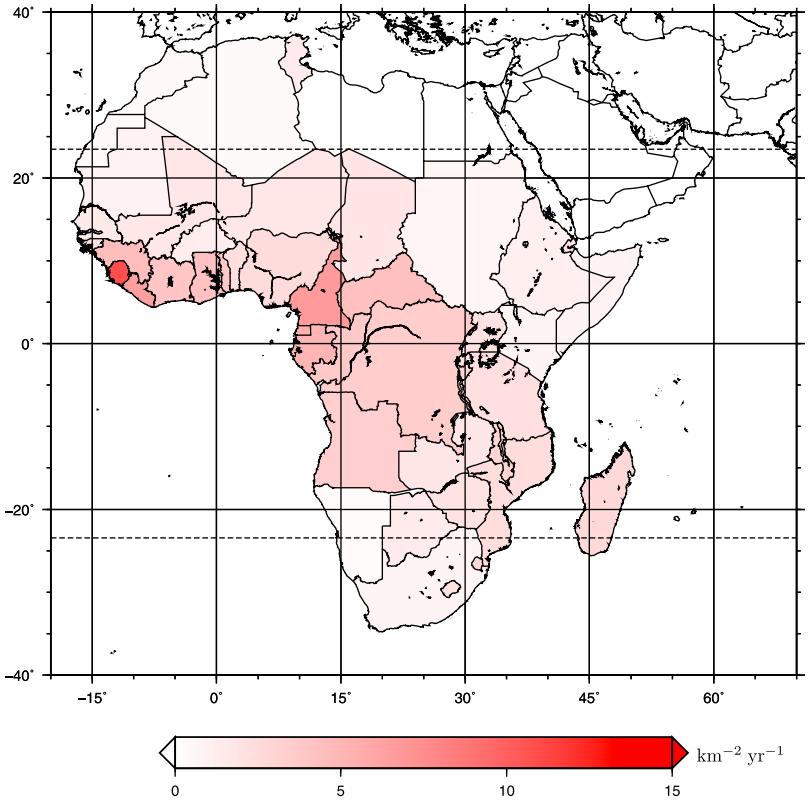

(a) amplitude, γ_2

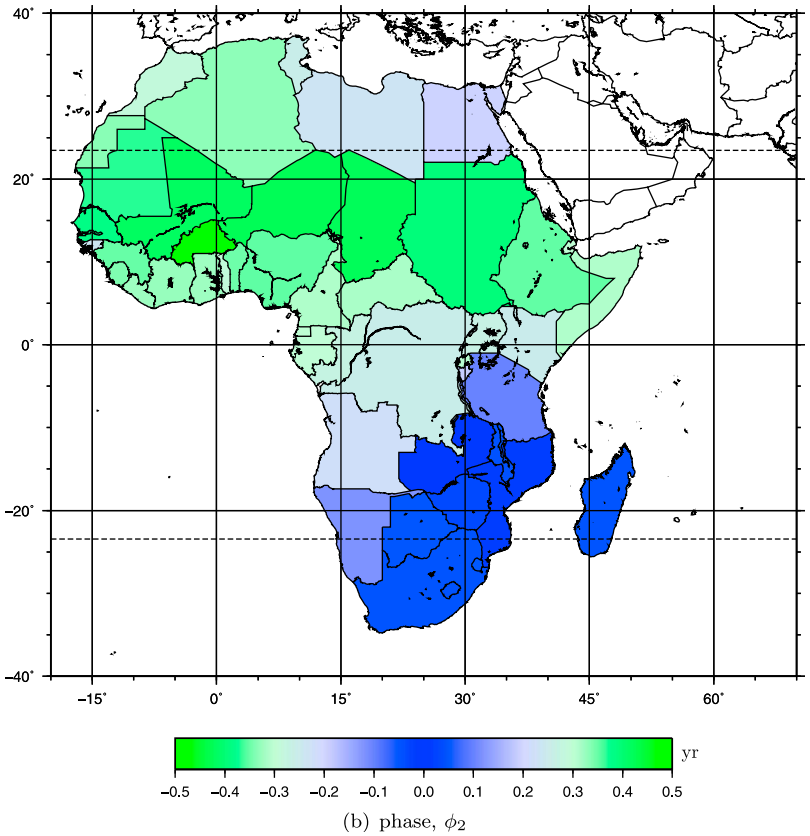

(b) phase, ϕ_2

Figure 4. Parameters for the semiannual component of total flash rate. Details as in Figure 3.

equator. Whereas, in the Southern Hemisphere, lightning exhibits a peak close to the Austral summer solstice, the peak in the Northern Hemisphere is delayed by 6 months and occurs around the boreal summer solstice. This pattern is consistent with the fact that lightning activity is most prevalent during the summer months. Although ϕ_1 for Egypt appears to be anomalous, being similar to values in the Southern Hemisphere, this arises because the amplitude of the annual variation is negligibly small and is thus insignificant.

[29] The definition of ϕ_2 is such that semiannual variations with $\phi_2 \approx 0.25$ are similar to those with $\phi_2 \approx -0.25$, and those with $\phi_2 \approx 0.5$ are similar to those with $\phi_2 \approx -0.5$. The domain $-0.5 \leq \phi_2 \leq 0.5$ is thus redundant. However, the values of ϕ_2 which are presented here represent the phase of the peak in the semiannual signal which is closest to the peak in the annual signal. This allows the superposition of the annual and semiannual components to be more readily interpreted. When considering the semiannual variation it is important to examine the phases from Figure 4b in conjunction with the amplitudes from Figure 4a, considering only those countries which exhibit a nonnegligible γ_2. Countries in North Africa have only rudimentary semiannual variations, $\gamma_2 \ll \gamma_1$, so that for these countries ϕ_2 is irrelevant. Countries with significant γ_2 are found in West, Central and Southern Africa. Mali, for example, has $\gamma_2 \sim \gamma_1$ and $\phi_2 \sim \phi_1$, so that the summer peak is sharpened. In contrast, Guinea has $\gamma_2 \sim \gamma_1$ but ϕ_2 and ϕ_1 differ by approximately 3 months so that the semiannual variation depresses the peak in the annual curve. A number of other countries conform to one of these extremes and the remainder are intermediate cases.

[30] Many countries located close to the equator exhibit two well defined peaks close to the equinoxes. In most cases the peak at the Vernal equinox is higher than that around the autumnal equinox. An example is Liberia as illustrated in Figure 1g. Notable exceptions are Tunisia and Uganda which are dominated by a peak during September. The relative amplitude of the two lightning peaks for Liberia is echoed by peaks in the monthly mean precipitation for neighboring Côte d'Ivoire, both of which occur during periods when the potential temperature decreases with height, indicating favorable conditions for strong convection [*Zhang et al.*, 2006, Figure 6].

3. Discussion

[31] The analysis in section 2 isolated some general trends in the cycles of lightning activity for countries in Africa. A broad distinction can be made between the lightning patterns for tropical and subtropical countries, where the former display a more significant semiannual variation. Outside the tropics, where the contribution of the semiannual component is small, the annual peak flash rate is approximately $\alpha + \gamma_1$, occurring on a date close to ϕ_1. Within the tropics, there is a monotonic decrease in γ_1/α approaching the equator, indicating that there is sustained activity throughout the year and seasonal variability is less important. The influence of the semiannual variation, characterized by γ_2/γ_1, increases north of the equator. This is probably attributable to motion of the ITCZ over the Gulf of Guinea.

[32] To place these results into context, Figure 5 presents the mean annual latitudinal variation in lightning flash rate density averaged zonally across the African continent. Figure 5 is analogous to Figure 9a of *Christian et al.* [2003], but confined to the African landmass. The annual migration of peak lightning activity back and forth across the equator is conspicuous, being mostly south of the equator around December and north of the equator around June. The dearth of lightning north of 12°N is readily apparent. This corresponds to the southern extremity of the Sahara and is consistent with the northern boundaries for appreciable values of α and γ_1 reflected in Figures 1 and 2a. The dominance of the Congo River Basin, heightened between January and March but present throughout the year, is also evident and is in accord with the time series displayed in Figure 1h. The isolated region of activity centered on 10°N between May and October occurs when the ITCZ has reached its northern extreme and lightning over the Congo River Basin is at a minimum. Similarly, the island of activity centered on 28°S in December and January corresponds to peak summer lightning incidence in Southern African countries.

3.1. Cluster Analysis

[33] A cluster analysis was performed to obtain an overview of the data presented in Table 1. The annual pattern of lightning occurrence for each country was first centered and normalized, then a dissimilarity matrix was constructed using the Euclidean metric. A hierarchical cluster analysis using the single (minimum distance) linkage method resulted in the dendrogram presented in Figure 6. The tree was cut at a level yielding 7 distinct groups. Group 1, containing only Egypt, could be immediately ignored since lightning was too scarce in this region to obtain meaningful statistics.

[34] Group 2, consists of Ghana and Côte d'Ivoire, which are adjacent to the Gulf of Guinea, and Somalia, which is located in the Horn of Africa. Although these countries are located on opposite sides of the continent, they all have $\overline{\lambda} \simeq$ 7°N and an annual variation which has a major peak during May, followed by a minor peak in October.

[35] Sierra Leone, which is the only member of group 3, is located in West Africa at 8.6°N, bordering on the Atlantic Ocean. It also has a bimodal annual lightning distribution with peaks of roughly equal height in May and October, a minor minimum in August and a major minimum in February.

[36] Group 4 comprises the rest of the African countries north of the equator, all of which experience maximum lightning activity in the middle of the year as exemplified by Figure 1c. There are a few distinct subgroups. Uganda and Tunisia, where the former is equatorial and the latter borders the Mediterranean Sea, have a major peak in September preceded by a shoulder in May, as illustrated in Figure 1a. Nigeria and Benin have peaks which are skewed toward the beginning of the year, as portrayed by Figure 1e. Guinea and the Central African Republic, although geographically distant, both have a broad maximum with an oblique top as illustrated in Figure 1d. Togo and Cameroon, both of which border on the Gulf of Guinea, are bimodal but the discrepancy between the peaks is not as pronounced as for group 2.

[37] Kenya and Liberia, which are the sole members of groups 5 and 6, respectively, also exhibit a bimodal varia-

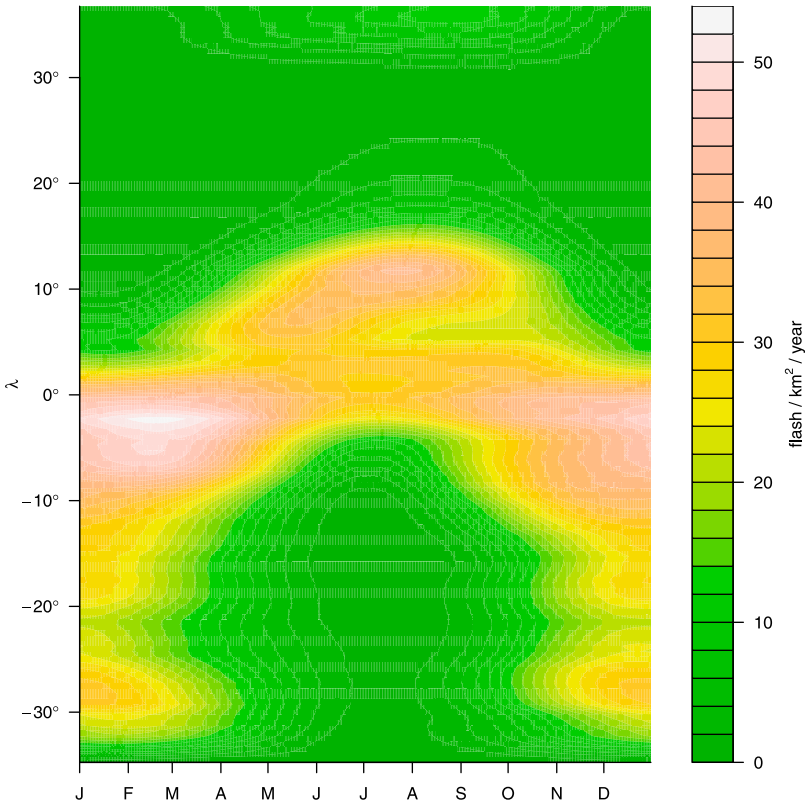

Figure 5. Mean annual variation in HRAC LIS/OTD flash rate density averaged zonally across the African continent.

tion, but this might more appropriately be described as dipolar, with a maximum in April descending rapidly to a minimum in August and then recovering to another minor peak in the latter half of the year. This pattern is demonstrated in Figure 1g.

[38] The countries in group 7 are located in the Southern Hemisphere and are characterized by peak activity at either the end or beginning of the year. Neighboring countries, the Democratic Republic of the Congo and Angola, have a broad maximum extending from November to February, as shown in Figure 1h. Rwanda is similar but the maximum is shifted a few weeks earlier in the year. The Republic of the Congo, Equatorial Guinea and Gabon, which are all located east of the Democratic Republic of the Congo and border on the Atlantic Ocean, form a clear subgroup with a single maximum in March, dropping rapidly to a minimum in July and recovering more gradually in the latter half of the year. The rest of the countries in this group have unimodal patterns with maxima between December and February.

[39] The classification scheme presented in Figure 6 does not necessarily reflect groups with similar climates as defined by the Köppen-Geiger climate classification system

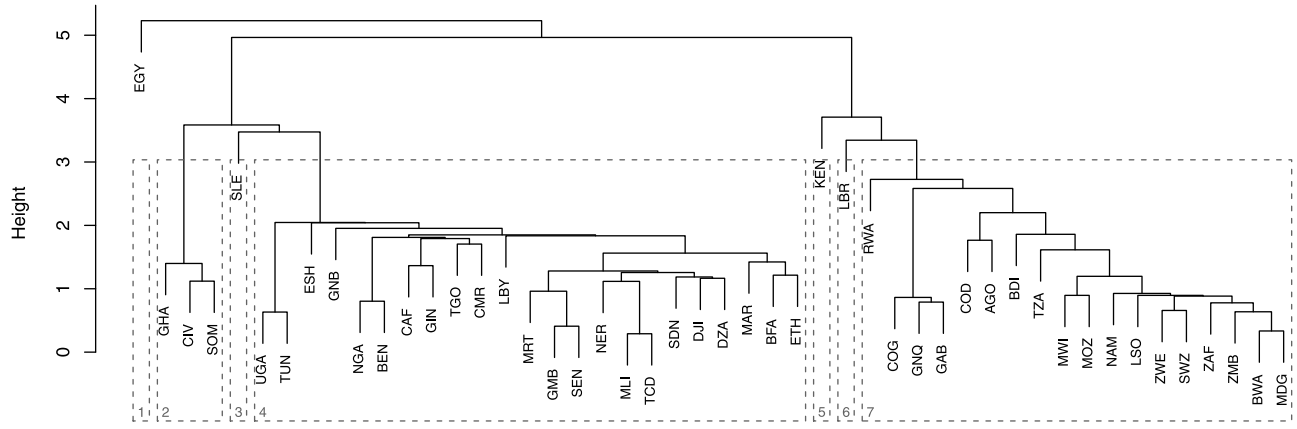

Figure 6. Cluster analysis of the annualized total flash rate density variation. The metric is the Euclidean distance between the normalized mean annual variations. The tree was cut at a level yielding seven distinct groups, which are labeled in grey.

[*Kottek et al.*, 2006]. Liberia and Kenya, for example, represent different climate regimes, where the former is entirely tropical (Köppen-Geiger group A), while the latter encompasses tropical, dry (Köppen-Geiger group B) and temperate (Köppen-Geiger group C) climates. A cluster within group 7 consists of countries in Southern Africa which include various climatic regimes. Group 7 also includes countries closer to the equator which have a tropical climate. Group 4 is populated by countries which are either tropical or dry. This group therefore characterizes two profoundly different climates but which have similar annual patterns of lightning activity.

3.2. Effect of the African Monsoon

[40] The West African monsoon consists of enhanced precipitation associated with a change in wind direction. It is caused by the seasonal cycle in land temperature relative to that of the Atlantic Ocean, which creates a thermal low pressure over the land during summer, leading to south westerly onshore transport of moist air, and the converse during winter. The peak of the West African monsoon occurs in July or August, and this corresponds to the principal maxima in lightning activity observed in many countries in North and West Africa.

[41] The West African monsoon has been found to consist of two distinct phases [*Gu et al.*, 2004; *Gu and Adler*, 2004]. During the first stage in early Boreal summer (December to February) the monsoon is focused off the Guinean coast around 5°N. The second stage, starting in the Boreal spring, is characterized by an intensification and a northward shift to around 10°N. The first and second stages of the monsoon are illustrated by the shift in peak lightning activity between Nigeria (Figure 1e) and Mali (Figure 1b). Whereas the former is more affected by the first stage of the monsoon in early summer, the peak in lightning activity is delayed in the latter country, which is dominated by the second phase of the monsoon. Observations of the monsoon rain band are generally made over land and the extrapolation of these measurements to neighboring marine environments can be problematic since they represent a different climate regime.

[42] It is interesting to note that the winds responsible for the West African monsoon differ from those which are associated with the ITCZ. The conventional location for the ITCZ is at the confluence of the northeasterly and southeasterly trade winds blowing from the Northern and Southern Hemisphere, respectively, whereas the West African monsoon winds are southerly or southwesterly. These winds are active throughout the year but exhibit a clear seasonal cycle, reaching a peak between July and September [*Zhang et al.*, 2006].

3.3. ITCZ

[43] The key to an understanding of the weather and climate in Nigeria and neighboring countries farther west along the coast is the annual migration of the ITCZ and the associated belt of cloud, heavy rain, high humidity and relatively low temperature. The ITCZ, which transects equatorial Africa, occurs at the convergence of the trade winds blowing from the Northern and Southern Hemispheres. In West Africa the northeasterly trade winds are dry and bring higher temperatures, while the winds from the Gulf of Guinea are moist. Drier and sunnier weather, with higher temperatures, prevails on the northern side of the ITCZ, and squall lines play an important role in precipitation and lightning activity [*Fernandez*, 1982]. A belt of cloud and rain lies on the southern side of the ITCZ. The ITCZ lies over or near the Guinean coast in December and January and moves north to about 20°N by July and August. It then returns southward rather more rapidly between September and December. Much of Nigeria and the region to the west experience two rainy periods as the ITCZ moves north or south. Farther north the two rainy seasons merge to give a single wet season between July and September. The West African monsoon is strongly related to the latitudinal motion of the ITCZ.

[44] The low-level convergence associated with the ITCZ leads to vigorous convection and the formation of thunderclouds. The seasonal migration of the ITCZ therefore has an appreciable influence on tropical lightning. In West Africa the ITCZ is north of the equator throughout the year, while over East Africa it exhibits a larger latitudinal range, roaming deep into the Southern Hemisphere. Countries like Mali, Niger, Nigeria and Sudan experience maximum lighting activity at midsummer when the ITCZ has reached its northernmost position, and an almost complete lack of lightning at midwinter. The converse applies in Zambia and the United Republic of Tanzania which are exposed to peak lightning activity when the ITCZ attains is southernmost extreme.

[45] The asymmetry between the two flash rate peaks in Figure 1g clearly demonstrates the effect of the ITCZ. The latitude of Liberia (6.4°N) is such that the Sun is located close to the zenith twice during the year. There should therefore be two peaks in the solar input. However, it appears that only the first translates directly into enhanced lightning activity (where the lightning peak occurs during the northward passage of the Sun through the zenith in spring), while the second peak is shallower and starts during autumn and extends into winter. The disparity between the peaks may be associated with the annual migration of the ITCZ since the northward motion is gradual, and the ITCZ is thus active over Liberia for an extended period during the first half of the year, while the southward passage is more abrupt, and Liberia is thus exposed to the ITCZ for only a short period during the second half of the year. The contrast between the northward and southward motion of the ITCZ is probably due to the thermal inertia of the waters of the Gulf of Guinea which retard the ITCZ motion, causing it to lag behind the Sun as it moves northward across the equator. The asymmetry between the two peaks may also be associated with the occurrence of the long and short rains [*Levinson*, 2005].

3.4. The Sahara

[46] The Sahara covers most of North Africa, extending over a significant fraction of Chad, Egypt, Libya, Mali, Mauritania, Morocco, Niger, Western Sahara, Sudan and Tunisia. Due to the lack of water vapor, lightning is scarce over these desert regions, where α is small [*Sparrow and Ney*, 1971]. The flash rates in Libya and Egypt, and to a lesser extent Morocco and Tunisia, are so low that a reliable pattern of occurrence may not be obtained from satellite sampling. However, with the exception of Egypt these countries still exhibit a credible annual cycle.

3.5. The Sahel

[47] The Sahara is bounded to the south by the Sahel, which is a transitional belt of semiarid tropical savannas and grasslands. The Sahel encompasses portions of Senegal, Mauritania, Mali, Burkina Faso, Niger, Nigeria, Chad and Sudan. Lightning activity within the Sahel is intermediate between the dearth of North Africa and the profusion of Central Africa. Maxima are attained midyear and the semiannual component makes only a relatively small contribution.

[48] *Laing and Fritsch* [1993] found that the majority of African Mesoscale Convective Complex (MCC) activity originated in the Sahel, and that the characteristics of MCC over Africa are similar to those elsewhere, being both nocturnal and initially continental or coastal. The frequency and mean latitude of MCC were observed to depend on solar insolation, with a peak in activity during the Northern Hemisphere summer and reduced frequency south of the equator [*Laing and Fritsch*, 1993, Figure 7]. Sahelian MCC migrate toward the Atlantic Ocean, and some develop into hurricanes.

3.6. Tropical Africa

[49] The Sun's equinoctial crossings of the equator lead to a subtle enhancement of surface air temperature. This causes a biannual elevation in tropical convection, and hence lightning activity. The peaks in tropical lightning activity do not necessarily occur at the equinoxes. This is probably due to the influence of the oceans. Since land is more responsive to solar insolation, areas which are remote from the oceans will respond most rapidly to the seasonal change in the Sun's declination, while regions which are close to the oceans may experience a delay induced by the thermal inertia of the oceans.

[50] The lightning activity in countries immediately north of the Gulf of Guinea is characterized by a strong semiannual component. The pattern of occurrence has minima in July-August and December–February and its form can be explained as follows: weather in the neighborhood of the Gulf of Guinea is strongly influenced by a warm dry northeasterly wind meeting a cooler moist southwesterly wind blowing in from the Atlantic Ocean. These winds meet at the ITCZ, which should provide ideal conditions for thunderstorm creation. The ITCZ lies close to the equator in December and January, giving warm dry conditions to the north. It moves northward reaching a latitude of about 20°N in July and August before moving south again. This migration should correspond to a moving band of thunderstorms giving two maxima in occurrence over a given country. This is illustrated by the pattern of occurrence for Liberia and Sierra Leone in Figure 1. Close to the equator the annual rainfall pattern is also bimodal, with peaks during March-April and October-November [*Kazadi and Kaoru*, 1996]. The lightning maxima then coalesce into one, as the ITCZ reaches its most northern latitude, producing a single peak in July and August. This is evident in the pattern of occurrence for Mali and Niger in Figure 1.

[51] The most intense lightning activity over Africa occurs in the Democratic Republic of the Congo, which lies entirely within the Congo River Basin, a vast region covered by lush tropical rain forests. *Williams and Sátori* [2004] found that the frequency of lightning over the Congo River Basin exceeded that over the Amazon River Basin by a factor of around 2.8. This contrast could not be explained in terms of thermodynamic conditions, which differed only slightly between these two major drainage basins, and *Williams and Sátori* [2004] thus hypothesized that aerosol loading might play a significant role. In both locations biomass burning is the principal source of aerosols. The resulting smoke causes increased convective activity as a result of cloud microphysics, which is balanced by decreased convection due to the associated radiative effect [*Altaratz et al.*, 2010]. Fires are most prevalent in the Congo River Basin during the middle of the year when the levels of lightning are at their minimum [*Williams and Sátori*, 2004, Figure 10]. Satellite observations of aerosol optical depth [*Chu et al.*, 2002] indicate that Africa is the most polluted on a continental scale. High aerosol loadings inhibit the formation and coagulation of smaller cloud droplets, suppressing precipitation and allowing the droplets to ascend to greater heights within clouds where they participate in charge separation [*Williams et al.*, 2002; *Saunders*, 2008].

[52] The climate and vegetation of the Democratic Republic of the Congo is determined by its location beneath the ITCZ. The annual temperature range is relatively low (less than 2°C) over most of the country, and is thus not a meaningful parameter for the definition of seasons, which are more appropriately identified as either rainy or dry [*Kazadi and Kaoru*, 1996]. Furthermore, there is evidence to suggest that over decadal time scales the temperature over the Democratic Republic of the Congo is gradually escalating, while the precipitation rate is declining [*Kazadi and Kaoru*, 1996]. The average annual variation in lightning over the Democratic Republic of the Congo is plotted in Figure 1h, which compares favorably with the monthly averages of *Williams and Sátori* [2004, Figure 1], where an extended period of sustained high lightning activity was also identified from September to April. There is a relatively small variation around the mean of $\alpha = 47.8\ \mathrm{km^{-2}\ yr^{-1}}$, with the amplitudes of the annual and semiannual components being 9.7 and 3.5 $\mathrm{km^{-2}\ yr^{-1}}$, respectively, so that $\gamma_2/\gamma_1 = 0.37$. The semiannual behavior, with peaks around the equinoxes, is also reflected in the river discharge record of the Congo River Basin [*Williams and Sátori*, 2004]. Even the minimum level of activity during June and July is rather vigorous. The consistently high activity is mostly due to the sustained levels of temperature and humidity. The Democratic Republic of the Congo therefore provides the principal source of terrestrial lightning activity and maintains this role throughout the year.

[53] Sudan is the largest country in Africa, with an area of $2.51 \times 10^6\ \mathrm{km^{-2}}$. It lies entirely within the tropics between 3.8°N and 22.8°N. The northern part of Sudan is desert, with a parched climate similar to that of the Sahara. Dry northeasterly winds prevail here for most of the year. Southward the country becomes progressively less arid. Southerly and southwesterly winds transport moist air from the Atlantic Ocean and Congo River Basin, bringing rain. The rainy season extends from April to October. Maximum temperatures are achieved in July and August. Airborne dust from the Sahara can have an appreciable impact on conditions in Sudan [*Idso and Brazel*, 1977; *von Hoyningen-Huene et al.*, 1999], and haboobs often precede thunderstorms. As indicated in Figure 1c, Sudan experiences maximum

lightning activity between July and September, when temperature and humidity are high. Most of the lightning is focused in the south of the country.

3.7. Subtropical Southern Africa

[54] In Southern Africa (South Africa, Lesotho, Botswana, Malawi, Zambia, Swaziland and Zimbabwe) the variation is well described by a simple sinusoid. The phase is such as to produce maxima shortly after the summer solstice when temperature and humidity are high.

3.8. Other Influences

[55] The oceans exercise a considerable influence on the lightning activity of the adjacent land. *Petersen and Rutledge* [2001] identified three regimes of oceanic influence: isolated oceanic locations, coastal areas and interior continental regions. Interior regions could be either oceanic (for example, the Amazon River Basin) or continental (for example, the Congo River Basin) in nature. Coastal areas could vary between oceanic or continental on a seasonal time scale. In all cases the degree of oceanic influence strongly determined convective vigor and the intensity of associated lightning. Namibia is bordered to the west by the cold Benguela Current which suppresses lightning activity along the coastal zone. The Benguela Current also influences the west coast of South Africa. The warm Guinea Current which flows down the coast of West Africa and into the Gulf of Guinea is responsible for providing the warm moist air which drives the West African monsoon. Similarly, the warm Agulhas and Mozambique Currents, which flow down the east coast of Southern Africa are also sources of warm moist air. Exceptions are Somalia and Kenya, both of which are adjacent to warm ocean currents yet experience only a marginal level of lightning activity.

[56] Over interannual time scales a relationship has been found between temperature anomalies and ENSO [*Kazadi and Kaoru*, 1996], which may exert an influence on the interannual variability in lightning occurrence. *LaJoie and Laing* [2008] found that lightning along the Gulf Coast was enhanced during the ENSO warm phase, but depressed during the cool or neutral phase. Furthermore, winter lightning was found to be especially sensitive to ENSO. The regional models provided in this analysis provide a baseline against which variations in lightning activity, possibly related to ENSO or other phenomena, might be compared.

[57] It is interesting to speculate about a possible link between lightning occurrence and vegetation. Certainly in the arid expanses of North Africa there is negligible vegetation and lightning is scarce, while closer to the equator profuse lightning occurs over a verdant landscape. There is evidence to suggest that low levels of lightning are associated with bare ground, but that lightning becomes more frequent in wooded areas [*Kotroni and Lagouvardos*, 2008], where the latter are perhaps more conducive to lightning activity since they retain moisture more readily and thus act as a reservoir for humidity. Furthermore, the albedo of vegetation is usually lower than that of soil [*Samain et al.*, 2008]. The meagre levels of lightning over Somalia and Kenya, both of which are tropical and adjacent to a warm ocean current, is in keeping with the fact that the dominant vegetation in this region is semidesert or steppes. *Kilinc and Beringer* [2007], however, found that the lightning density increased from woodland to shrub to grassland, suggesting that the distinction may arise from differences in surface heating. The possible relationship between lightning and vegetation appears to be bidirectional since the prevalence of lightning may also determine the type of vegetation which flourishes in a particular area on the basis of its fire tolerance [*Manry and Knight*, 1986].

[58] Topography may also dictate the level of thunderstorm activity. Most of Lesotho lies at an altitude in excess of 1800 m and is generally cooler that other regions at the same latitude, yet it experiences an average flash rate density of α = 23.8 km^{-2} yr^{-1}. Ethiopia, although largely semidesert and steppes, has α = 23.8 km^{-2} yr^{-1} due to the pronounced effect of the highlands, most of which are above 1500 m. The relationship between elevated ground and lightning does not imply that the converse also holds. The Congo River Basin lies at relatively low altitude yet is the location of the Earth's most intense lightning activity. However, the mean elevation of the Congo River Basin is some 300–400 m higher than the Amazon River Basin, which might also account for the discrepancy in lightning activity [*Williams and Sátori*, 2004]. Furthermore there is an enhancement in lightning activity over the higher terrain on the eastern border of the Congo River Basin [*Williams and Sátori*, 2004]. In the absence of other factors such as heat and humidity, high ground is more conducive to lightning activity, perhaps due to the enhanced potential gradient between clouds and the ground.

4. Conclusion

[59] It has been argued that, at a given location, lightning activity increases with temperature and certainly some results [e.g., *Williams*, 1992; *Dinnes*, 1999] support this. However, the production of lightning requires a combination of factors, including humidity and surface warming sufficient to produce strong convection. There is, for example, very little or no lightning in the hot desert regions of North Africa. Vigorous lightning thus occurs in conjunction with high relative humidity, whereas in a dry climate there is very little lightning even at the hottest time of the year. It would seem, however, that in a given country where there is appreciable humidity, that a relationship between temperature and lightning may well be found.

[60] The relationship between lightning and temperature suggests that global lightning activity might be an indicator of climate change [*Williams*, 1992; *Bering*, 1995]. The simple conclusion that lightning activity will increase with elevated global temperatures might be naive since it does not take into account the impact that a warmer Earth will have on relative humidity. In principle one should be able to extract a long-term trend from the LIS/OTD data. However, a preliminary analysis suggests that some neighboring countries within Africa are experiencing trends of opposite sign and it is thus likely that the length of the lightning time series is currently insufficient to generate robust statistics and justify a conclusion. The parameters presented here represent entire countries, each of which may be composed of a range of climatic regimes. Therefore it is feasible that opposite climate trends in different portions of a particular country may result in a negligible net change in the corresponding lightning parameters.

[61] Political boundaries yield a somewhat artificial partitioning of lightning data. The associated spatial resolution is also rather coarse. Climatology data are commonly presented on a 5° by 5° grid [*Jones and Moberg*, 2003], which, although regular, does not present significantly finer spatial detail. Furthermore, it might be argued that lightning data averaged over whole countries does not represent the sometimes considerable regional variations within those countries. For example, South Africa and Sudan are large and encompass a range of climate regimes. South Africa has abundant lightning on the Highveld but little lightning in the Western Cape. The north of Sudan is dry with scarce lightning, while thunderstorm activity becomes more profuse farther south. In both cases the data for the whole country represent an average of the two extremes. This leads to the spurious discrepancies between adjacent countries. For example, Lesotho has significantly higher average activity than South Africa, but has lightning conditions which are comparable to the adjacent areas in South Africa. However, this analysis is meaningful when compared to annual climatologies of other meteorological parameters like temperature, relative humidity and precipitation, which are often presented as an average over an entire country.

[62] The analysis presented here reduces the description of the annual variation in lightning activity for each country in Africa to a set of five parameters. The average lightning intensity is described by α. The variability around α is characterized by γ_1 and γ_2, the amplitudes of the annual and semiannual cycles. The depth of the seasonal cycle is reflected by γ_1. Outside the tropics γ_2 is negligible, but becomes more important closer to the equator. The relative phase of the annual and semiannual variations is determined by ϕ_1 and ϕ_2, where the combined signal can range from either a sharpened or flattened unimodal to a symmetrical bimodal variation. This simple parameterization facilitates a comparison of the temporal variation in lightning activity. Furthermore, it also establishes a baseline against which the observations for a given year can be compared in order to identify anomalous activity.

[63] It would be advantageous to validate the parameters derived here against an independent data set, preferably one derived from a regional lightning detection network which affords both high spatial and temporal resolution. Such a network is operated within South Africa, however, the spatial coverage of the network is not uniform, being strongly biased toward the South African Highveld. Nevertheless, since this is the location of the majority of South African lightning, a comparison against these data would still be meaningful.

[64] **Acknowledgments.** We appreciate useful discussions with Agatha de Boer (School of Environmental Science, University of East Anglia, Norwich, United Kingdom). The LIS/OTD HRAC data were produced by the LIS/OTD Science Team (Principal Investigator Hugh J. Christian, NASA/Marshall Space Flight Center) and were obtained from the Global Hydrology Research Center (http://ghrc.msfc.nasa.gov/).

References

Altaratz, O., I. Koren, Y. Yair, and C. Price (2010), Lightning response to smoke from Amazonian fires, *Geophys. Res. Lett.*, *37*, L07801, doi:10.1029/2010GL042679.

Baker, M. B., A. M. Blyth, H. J. Christian, J. Latham, K. L. Miller, and A. M. Gadian (1999), Relationships between lightning activity and various thundercloud parameters: Satellite and modelling studies, *Atmos. Res.*, *51*(3–4), 221–236, doi:10.1016/S0169-8095(99)00009-5.

Bengtsson, L. (2006), On the response of the climate system to solar forcing, *Space Sci. Rev.*, *125*, 187–197, doi:10.1007/s11214-006-9056-3.

Bering, E. A. (1995), The global circuit: Global thermometer, weather byproduct or climatic modulator?, *Rev. Geophys.*, *33*(S1), 845–862, doi:10.1029/95RG00549.

Blumenthal, R. (2005), Lightning fatalities on the South African highveld: A retrospective descriptive study for the period 1997 to 2000, *Am. J. Forensic Med. Pathol.*, *26*(1), 66–69, doi:10.1097/01.paf.0000154115.12168.46.

Boccippio, D. J., W. J. Koshak, and R. J. Blakeslee (2002), Performance assessment of the optical transient detector and lightning imaging sensor. Part I: Predicted diurnal variability, *J. Atmos. Oceanic Technol.*, *19*(9), 1318–1332, doi:10.1175/1520-0426(2002)019<1318:PAOTOT>2.0.CO;2.

Brooks, C. E. P. (1934), The variation of the annual frequency of thunderstorms in relation to sunspots, *Q. J. R. Meteorol. Soc.*, *60*, 153–166, doi:10.1002/qj.49706025407.

Calogovic, J., C. Albert, F. Arnold, J. Beer, L. Desorgher, and E. O. Flueckiger (2010), Sudden cosmic ray decreases: No change of global cloud cover, *Geophys. Res. Lett.*, *37*, L03802, doi:10.1029/2009GL041327.

Carslaw, K. S., R. G. Harrison, and J. Kirkby (2002), Cosmic rays, clouds, and climate, *Science*, *298*, 1732–1737, doi:10.1126/science.1076964.

Carte, A. E., and R. E. Kidder (1977), Lightning in relation to precipitation, *J. Atmos. Terr. Phys.*, *39*(2), 139–148, doi:10.1016/0021-9169(77)90107-6.

Christian, H. J., et al. (2003), Global frequency and distribution of lightning as observed from space by the Optical Transient Detector, *J. Geophys. Res.*, *108*(D1), 4005, doi:10.1029/2002JD002347.

Chronis, T., E. Anagnostou, and E. Williams (2006), Lightning as an indicator of tropical cyclogenesis in African easterly waves, *Eos Trans. AGU*, *89*(47), Fall Meet. Suppl., Abstract AE43A-06.

Chu, D. A., Y. J. Kaufman, C. Ichoku, L. A. Remer, D. Tanré, and B. N. Holben (2002), Validation of MODIS aerosol optical depth retrieval over land, *Geophys. Res. Lett.*, *29*(12), 8007, doi:10.1029/2001GL013205.

Coates, L., R. Blong, and F. Siciliano (1993), Lightning fatalities in Australia, 1824–1991, *Nat. Hazards*, *8*(3), 217–233, doi:10.1007/BF00690909.

Collier, A. B., A. R. W. Hughes, J. Lichtenberger, and P. Steinbach (2006), Seasonal and diurnal variation of lightning activity over southern Africa and correlation with European Whistler observations, *Ann. Geophys.*, *24*(2), 529–542, doi:10.5194/angeo-24-529-2006.

Curran, E. B., R. L. Holle, and R. E. López (2000), Lightning casualties and damages in the United States from 1959 to 1994, *J. Clim.*, *13*(19), 3448–3464, doi:10.1175/1520-0442(2000)013<3448:LCADIT>2.0.CO;2.

Dinnes, D. (1999), Blitzgefahrdung in Deutschland, Master's thesis, Meteorol. Inst., Univ. of Munich, Munich, Germany.

Dlamini, W. M. (2009), Lightning fatalities in Swaziland: 2000–2007, *Nat. Hazards*, *50*(1), 179–191, doi:10.1007/s11069-008-9331-6.

Dmowska, R., and B. Saltzman (Eds.) (1999), *Long-Range Persistence in Geophysical Time Series*, *Adv. Geophys.*, vol. 40, Academic, San Diego, Calif.

Elsom, D. M. (2001), Deaths and injuries caused by lightning in the United Kingdom: Analyses of two databases, *Atmos. Res.*, *56*(1–4), 325–334, doi:10.1016/S0169-8095(00)00083-1.

Fernandez, W. (1982), Environmental conditions and structure of the West African and Eastern Tropical Atlantic squall lines, *Arch. Meteorol. Geophys. Bioclimatol., Ser. A*, *31*(1–2), 71–89, doi:10.1007/BF02257743.

Füllekrug, M., and A. C. Fraser-Smith (1997), Global lightning and climate variability inferred from ELF magnetic field variations, *Geophys. Res. Lett.*, *24*(19), 2411–2414.

Füllekrug, M., C. Price, Y. Yair, and E. R. Williams (2002), Intense oceanic lightning, *Ann. Geophys.*, *20*(1), 133–137.

Goldenberg, S. B., and L. J. Shapiro (1996), Physical mechanisms for the association of El Niño and West African rainfall with Atlantic major hurricane activity, *J. Clim.*, *9*(6), 1169–1187, doi:10.1175/1520-0442(1996)009<1169:PMFTAO>2.0.CO;2.

Gu, G., and R. F. Adler (2004), Seasonal evolution and variability associated with the West African Monsoon System, *J. Clim.*, *17*(17), 3364–3377, doi:10.1175/1520-0442(2004)017<3364:SEAVAW>2.0.CO;2.

Gu, G., R. F. Adler, G. J. Huffman, and S. Curtis (2004), African easterly waves and their association with precipitation, *J. Geophys. Res.*, *109*, D04101, doi:10.1029/2003JD003967.

Holle, R. L. (2008), Annual rates of lightning fatalities by country, paper presented at 20th International Lightning Detection Conference, Vaisala, Tucson, Ariz.

Hsu, C.-P. F., and J. M. Wallace (1976), The global distribution of the annual and semiannual cycles in precipitation, *Mon. Weather Rev.*, *104*(9), 1093–1101, doi:10.1175/1520-0493(1976)104<1093:TGDOTA>2.0.CO;2.

Idso, S. B., and A. J. Brazel (1977), Planetary radiation balance as a function of atmospheric dust: Climatological consequences, *Science*, *198*, 731–733, doi:10.1126/science.198.4318.731.

Jayaratne, E. R., and V. Ramachandran (1998), A five-year study of lightning activity using a CGR3 flash counter in Gaborone, Botswana, *Meteorol. Atmos. Phys.*, *66*(3–4), 235–241, doi:10.1007/BF01026636, 1998.

Jones, P. D., and A. Moberg (2003), Hemispheric and large-scale surface air temperature variations: An extensive revision and an update to 2001, *J. Clim.*, *16*(2), 206–223.

Kazadi, S.-N., and F. Kaoru (1996), Interannual and long-term climate variability over the Zaire River Basin during the last 30 years, *J. Geophys. Res.*, *101*(D16), 21,351–21,360.

Kilinc, M., and J. Beringer (2007), The spatial and temporal distribution of lightning strikes and their relationship with vegetation type, elevation, and fire scars in the Northern Territory, *J. Clim.*, *20*(7), 1161–1173, doi:10.1175/JCLI4039.1.

Kotroni, V., and K. Lagouvardos (2008), Lightning occurrence in relation with elevation, terrain slope, and vegetation cover in the Mediterranean, *J. Geophys. Res.*, *113*, D21118, doi:10.1029/2008JD010605.

Kottek, M., J. Grieser, C. Beck, B. Rudolf, and F. Rubel (2006), World map of the Köppen-Geiger climate classification updated, *Meteorol. Z.*, *15*(3), 259–263, doi:10.1127/0941-2948/2006/0130.

Krider, E. P., R. C. Noggle, A. E. Pifer, and D. L. Vance (1980), Lightning direction-finding systems for forest fire detection, *Bull. Am. Meteorol. Soc.*, *61*(9), 980–986, doi:10.1175/1520-0477(1980)061<0980:LDFSFF>2.0.CO;2.

Kuleshov, Y., D. Mackerras, and M. Darveniza (2006), Spatial distribution and frequency of lightning activity and lightning flash density maps for Australia, *J. Geophys. Res.*, *111*, D19105, doi:10.1029/2005JD006982.

Laing, A. G., and J. M. Fritsch (1993), Mesoscale convective complexes in Africa, *Mon. Weather Rev.*, *121*(8), 2254–2263.

LaJoie, M., and A. Laing (2008), The influence of the El Niño–Southern Oscillation on cloud-to-ground lightning activity along the Gulf Coast. Part I: Lightning climatology, *Mon. Weather Rev.*, *136*(7), 2523–2542, doi:10.1175/2007MWR2227.1.

Levinson, D. H. (2005), State of the climate in 2004, *Bull. Am. Meteorol. Soc.*, *86*(6), S1–S86.

López, R. E., and R. L. Holle (1998), Changes in the number of lightning deaths in the United States during the twentieth century, *J. Clim.*, *11*(8), 2070–2077, doi:10.1175/1520-0442(1998)011<2070:CITNOL>2.0.CO;2.

López, R. E., R. L. Holle, T. A. Heitkamp, M. Boyson, M. Cherington, and K. Langford (1993), The underreporting of lightning injuries and deaths in Colorado, *Bull. Am. Meteorol. Soc.*, *74*(11), 2171–2178, doi:10.1175/1520-0477(1993)074<2171:TUOLIA>2.0.CO;2.

Mackerras, D., and M. Darveniza (1994), Latitudinal variation of lightning occurrence characteristics, *J. Geophys. Res.*, *99*(D5), 10,813–10,822.

Manry, D. E., and R. S. Knight (1986), Lightning density and burning frequency in South African vegetation, *Vegetatio*, *66*(2), 67–76.

Marsh, N. D., and H. Svensmark (2000), Cosmic rays, clouds, and climate, *Space Sci. Rev.*, *94*(1–2), 215–230, doi:10.1023/A:1026723423896.

Misra, V. (2010), Interaction of interannual and diurnal variations over equatorial Africa, *J. Geophys. Res.*, *115*, D01111, doi:10.1029/2009JD012512.

Mudelsee, M. (2002), TAUEST: A computer program for estimating persistence in unevenly spaced weather/climate time series, *Comput. Geosci.*, *28*(1), 69–72, doi:10.1016/S0098-3004(01)00041-3.

Nickolaenko, A. P., M. Hayakawa, and Y. Hobara (1999), Long-term periodical variations in global lightning activity deduced from the Schumann resonance monitoring, *J. Geophys. Res.*, *104*(D22), 27,585–27,591, doi:10.1029/1999JD900791.

Orville, R. E., and R. W. Henderson (1986), Global distribution of midnight lightning—September 1977 to August 1978, *Mon. Weather Rev.*, *114*(12), 2640–2653.

Petersen, W. A., and S. A. Rutledge (2001), Regional variability in tropical convection: Observations from TRMM, *J. Clim.*, *14*(17), 3566–3586, doi:10.1175/1520-0442(2001)014<3566:RVITCO>2.0.CO;2.

Pittock, A. B. (1978), Solar cycles and the weather: Successful experiments in autosuggestion?, in *Solar-Terrestrial Influences on Weather and Climate*, edited by B. M. McCormac and T. A. Seliga, pp. 181–191, D. Reidel, New York.

Price, C., and D. Rind (1994), Possible implications of global climate change on global lightning distributions and frequencies, *J. Geophys. Res.*, *99*(D5), 10,823–10,832, doi:10.1029/94JD00019.

Price, C., Y. Yair, and M. Asfur (2007), East African lightning as a precursor of Atlantic hurricane activity, *Geophys. Res. Lett.*, *34*, L09805, doi:10.1029/2006GL028884.

Reason, C. J. C., and M. Rouault (2002), ENSO-like decadal variability and South African rainfall, *Geophys. Res. Lett.*, *29*(13), 1638, doi:10.1029/2002GL014663.

Rorig, M. L., and S. A. Ferguson (2002), The 2000 fire season: Lightning-caused fires, *J. Appl. Meteorol.*, *41*(7), 786–791, doi:10.1175/1520-0450(2002)041<0786:TFSLCF>2.0.CO;2.

Samain, O., L. Kergoat, P. Hiernaux, F. Guichard, E. Mougin, F. Timouk, and F. Lavenu (2008), Analysis of the in situ and MODIS albedo variability at multiple timescales in the Sahel, *J. Geophys. Res.*, *113*, D14119, doi:10.1029/2007JD009174.

Sátori, G., and B. Zieger (1996), Spectral characteristics of Schumann resonances observed in central Europe, *J. Geophys. Res.*, *101*(D23), 29,663–29,669, doi:10.1029/96JD00549.

Saunders, C. P. R. (2008), Charge separation mechanisms in clouds, *Space Sci. Rev.*, *137*(1–4), 335–353, doi:10.1007/s11214-008-9345-0.

Saunders, C. P. R., W. D. Keith, and R. P. Mitzeva (1991), The effect of liquid water on thunderstorm charging, *J. Geophys. Res.*, *96*(D6), 11,007–11,017.

Soula, S., and S. Chauzy (2001), Some aspects of the correlation between lightning and rain activities in thunderstorms, *Atmos. Res.*, *56*(1–4), 355–373, doi:10.1016/S0169-8095(00)00086-7.

Sparrow, J. G., and E. P. Ney (1971), Lightning observations by satellite, *Nature*, *232*(5312), 540–541, doi:10.1038/232540a0.

Takahashi, T. (1978), Riming electrification as a charge generation mechanism in thunderstorms, *Journal of the Atmospheric Sciences*, *35*(8), 1536–1548.

von Hoyningen-Huene, W., K. Wenzel, and S. Schienbein (1999), Radiative properties of desert dust and its effect on radiative balance, *J. Aerosol Sci.*, *30*(4), 489–502, doi:10.1016/S0021-8502(98)00074-3.

Watkins, N. W., M. A. Clilverd, A. J. Smith, C. J. Rodger, N. A. Bharmal, and K. H. Yearby (2001), Lightning atmospherics count rates observed at Halley, Antarctica, *J. Atmos. Sol. Terr. Phys.*, *63*(10), 993–1003, 2001.

Wetli, C. V. (1996), Keraunopathology. An analysis of 45 fatalities, *Am. J. Forensic Med. Pathol.*, *17*(2), 89–98.

Williams, E. R. (1985), Large-scale charge separation in thunderclouds, *J. Geophys. Res.*, *90*(D4), 6013–6025, doi:10.1029/JD090iD04p06013.

Williams, E. R. (1992), The Schumann resonance: A global tropical thermometer, *Science*, *256*, 1184–1187, doi:10.1126/science.256.5060.1184.

Williams, E. R. (1994), Global circuit response to seasonal variations in global surface air temperature, *Mon. Weather Rev.*, *122*, 1917–1929.

Williams, E. R. (2005), Lightning and climate: A review, *Atmos. Res.*, *76*(1–4), 272–287, doi:10.1016/j.atmosres.2004.11.014.

Williams, E. R. (2009), The global electrical circuit: A review, *Atmos. Res.*, *91*(2–4), 140–152, doi:10.1016/j.atmosres.2008.05.018.

Williams, E. R., and N. Renno (1993), An analysis of the conditional instability of the tropical atmosphere, *Mon. Weather Rev.*, *121*(1), 21–36.

Williams, E. R., and G. Sátori (2004), Lightning, thermodynamic and hydrological comparison of the two tropical continental chimneys, *J. Atmos. Sol. Terr. Phys.*, *66*(13–14), 1213–1231, doi:10.1016/j.jastp.2004.05.015.

Williams, E. R., et al. (2002), Contrasting convective regimes over the Amazon: Implications for cloud electrification, *J. Geophys. Res.*, *107*(D20), 8082, doi:10.1029/2001JD000380.

Zhang, C., P. Woodworth, and G. Gu (2006), The seasonal cycle in the lower troposphere over West Africa from sounding observations, *Q. J. R. Meteorol. Soc.*, *132*, 2559–2582, doi:10.1256/qj.06.23.

A. B. Collier, Hermanus Magnetic Observatory, PO Box 32, Hermanus 7200, South Africa. (collierab@gmail.com)

A. R. W. Hughes, School of Physics, University of KwaZulu-Natal, Durban 4041, South Africa. (arthur.r.w.hughes@gmail.com)